iScience

CellPress
OPEN ACCESS

Article

Development of sensorimotor-visual connectome gradient at birth predicts neurocognitive outcomes at 2 years of age

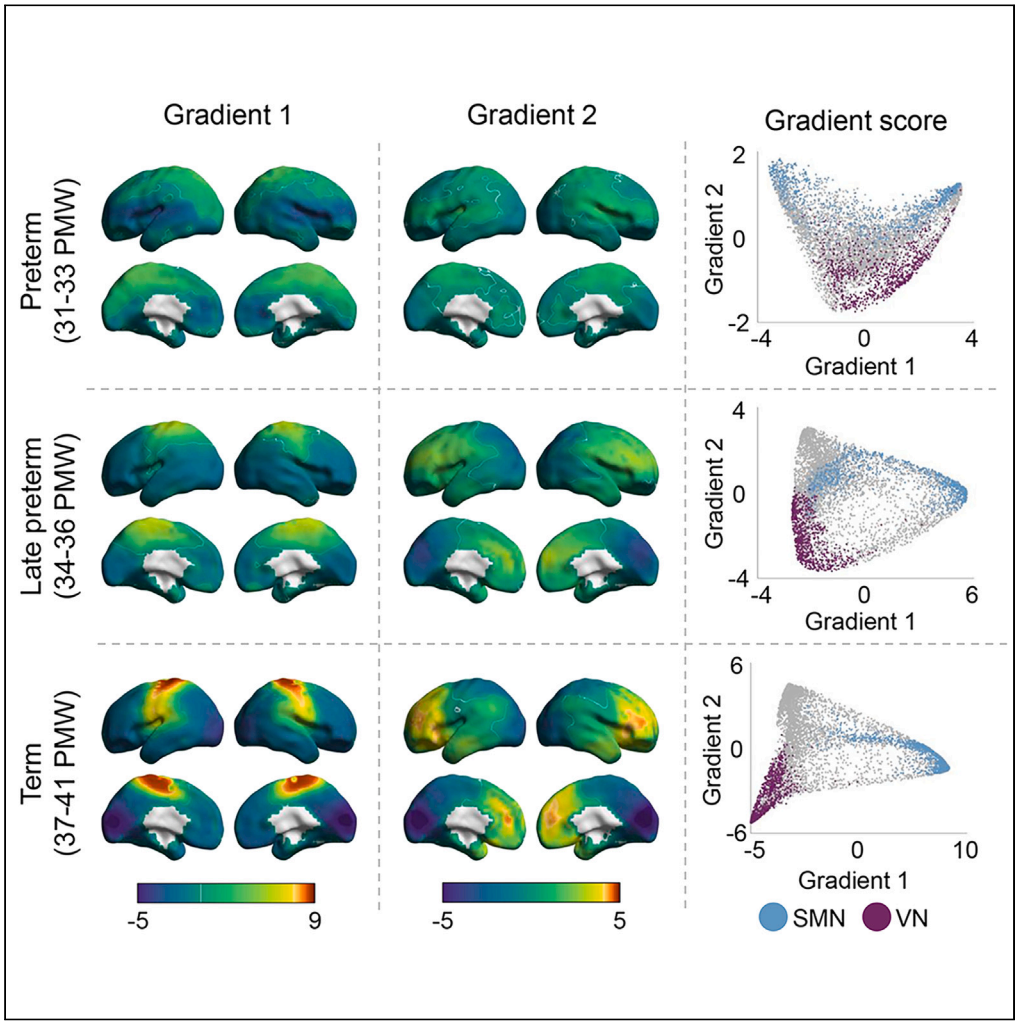

Yunman Xia, Jianlong Zhao, Yuehua Xu, ..., Nancy Rollins, Hao Huang, Yong He

huangh6@email.chop.edu (H.H.)
yong.he@bnu.edu.cn (Y.H.)

Highlights

Sensorimotor-to-visual gradient is present around the late preterm period

Global gradient structure substantially changes during the third trimester

Regional gradient develops mostly in the sensorimotor and visual regions

Sensorimotor-to-visual gradient at birth predicts cognitive outcomes at age 2

Xia et al., iScience *27*, 108981
February 16, 2024
https://doi.org/10.1016/j.isci.2024.108981

iScience

CellPress
OPEN ACCESS

Article

Development of sensorimotor-visual connectome gradient at birth predicts neurocognitive outcomes at 2 years of age

Yunman Xia,[1,2,3,4] Jianlong Zhao,[1,2,3] Yuehua Xu,[1,2,3] Dingna Duan,[1,2,3] Mingrui Xia,[1,2,3] Tina Jeon,[5] Minhui Ouyang,[5,8] Lina Chalak,[6] Nancy Rollins,[7] Hao Huang,[5,8,*] and Yong He[1,2,3,9,10,*]

SUMMARY

Functional connectome gradients represent fundamental organizing principles of the brain. Here, we report the development of the connectome gradients in preterm and term babies aged 31–42 postmenstrual weeks using task-free functional MRI and its association with postnatal cognitive growth. We show that the principal sensorimotor-to-visual gradient is present during the late preterm period and continuously evolves toward a term-like pattern. The global measurements of this gradient, characterized by explanation ratio, gradient range, and gradient variation, increased with age ($p < 0.05$, corrected). Focal gradient development mainly occurs in the sensorimotor, lateral, and medial parietal regions, and visual regions ($p < 0.05$, corrected). The connectome gradient at birth predicts cognitive and language outcomes at 2-year follow-up ($p < 0.005$). These results are replicated using an independent dataset from the Developing Human Connectome Project. Our findings highlight early emergent rules of the brain connectome gradient and their implications for later cognitive growth.

INTRODUCTION

The functional connectome of the adult human brain exhibits fundamental organizing principles, characterized by two core connectivity gradients, including the principal gradient from the primary sensorimotor and visual cortex to the transmodal regions and the secondary gradient separating the sensorimotor areas and visual cortex.[1,2] In recent years, significant research has focused on the primary-to-transmodal gradient in the adult brain connectome, highlighting its crucial implications for individual cognitive function[3,4] and mental health.[5,6] To date, the sensorimotor-to-visual gradient has received comparatively less attention. Studies in developmental populations have emphasized the importance of the sensorimotor-to-visual gradient in the neonatal brain[7,8] and that its dominance persists into late childhood.[9,10,11] However, the development of the sensorimotor-to-visual gradient during the prenatal period and its relationship with postnatal cognitive growth remain understudied.

The third trimester of pregnancy is a critical phase for the early development of cortical microstructures and functional organization in the human brain.[8,12–17] During this period, cortical neurons and neural circuits undergo rapid and significant growth, including the strengthening of axons,[18] the arborization of dendrites,[15] and the formation of synapses.[19] These microstructural changes primarily occur in the primary sensory and motor regions, which are associated with necessary cognitive functions after birth.[8,16,20,21] Functional connectomic studies have demonstrated prominent small-world properties, modular organization, and the emergence of hub regions primarily in the sensorimotor regions during the third trimester.[12,22] These findings suggest that the primary sensorimotor regions undergo remarkable development during this period. Recently, the sensorimotor-to-visual gradient has been observed in the neonatal brain.[7] We therefore hypothesize that the development of the sensorimotor regions during the third trimester drives the emergence and maturation of the sensorimotor-to-visual gradient, and that the development of this gradient provides a neural substrate to support cognitive growth in later life.

To test the above hypothesis, we collected task-free functional MRI (tf-fMRI) data in 39 neonates aged between 31 and 42 postmenstrual weeks (PMW) at the time of scanning, followed by cognitive assessment at a 2-year follow-up. Using functional connectome gradient

[1]State Key Laboratory of Cognitive Neuroscience and Learning, Beijing Normal University, Beijing 100875, China
[2]Beijing Key Laboratory of Brain Imaging and Connectomics, Beijing Normal University, Beijing 100875, China
[3]IDG/McGovern Institute for Brain Research, Beijing Normal University, Beijing 100875, China
[4]Institute of Science and Technology for Brain-Inspired Intelligence, Fudan University, Shanghai 200433, China
[5]Department of Radiology, Children's Hospital of Philadelphia, Philadelphia, PA 19104, USA
[6]Department of Pediatrics, University of Texas Southwestern Medical Center, Dallas, TX 75390, USA
[7]Department of Radiology, University of Texas Southwestern Medical Center, Dallas, TX 75390, USA
[8]Department of Radiology, University of Pennsylvania, Philadelphia, PA 19104, USA
[9]Chinese Institute for Brain Research, Beijing 102206, China
[10]Lead contact
*Correspondence: huangh6@email.chop.edu (H.H.), yong.he@bnu.edu.cn (Y.H.)
https://doi.org/10.1016/j.isci.2024.108981

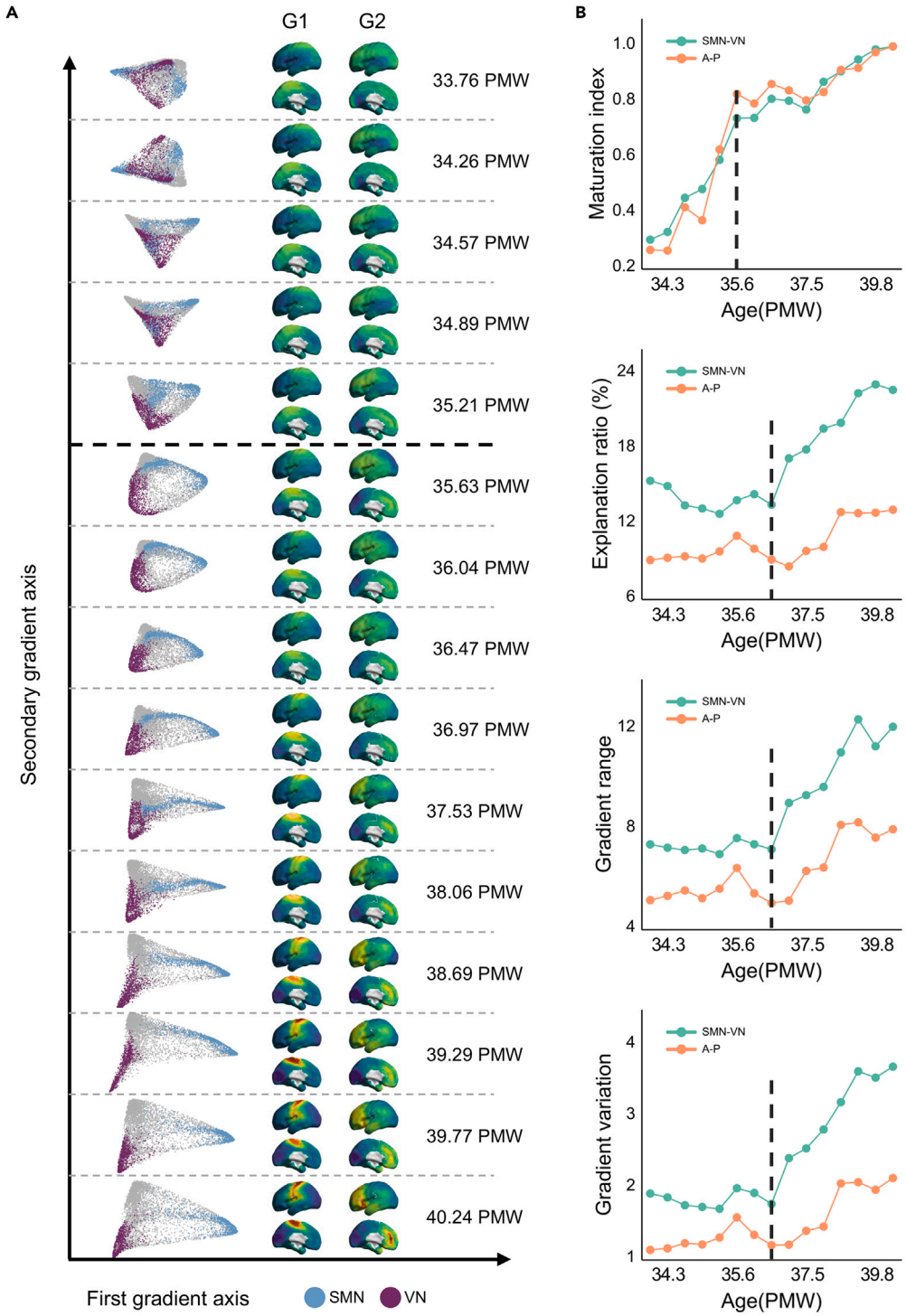

Figure 1. Connectome gradients of the human brain during the third trimester

(A) Functional connectome core gradients of 15 age windows, spanning from 33.76 to 40.24 postmenstrual weeks (PMW). In the scatterplots, the *x axis*, and *y axis* represent the scores of the first gradient and secondary gradient axis respectively, and the voxels within sensorimotor regions and visual regions were labeled by blue and purple. At the age window of 35.63 PMW, the sensorimotor-to-visual gradient is first observed, indicated by the voxels within the sensorimotor area (*blue*) and visual cortex (*purple*) initially occupying the extreme locations of the first gradient axes. Subsequently, this gradient organization gradually enlarges the ranges along the first gradient axes after this window. The anterior-to-posterior gradient is first observed at the approximate age window of

Figure 1. *Continued*

34.57 PMW, characterized by the voxels within the visual cortex (*purple*) clustered at the extremes of the second gradient axes. G1 means the first gradient, while G2 indicated the secondary gradient.

(B) The maturation index and global measures of both gradients across age windows. At the age window of 35.63 PMW, the maturation index of both gradients experiences a significant surge from approximately 0.5 to 0.8, and remains at a high level thereafter. After one week of 35.63 PMW, i.e., the age window of 36.47 PMW, the sensorimotor-to-visual gradient exhibits substantial increases in the explanation ratio, gradient range, and gradient variation, while these metrics remain relatively stable before this age. Moreover, the anterior-to-posterior gradient also demonstrates slight increases in these global measures. SMN-VN means the sensorimotor-to-visual gradient, while A-P indicated the anterior-to-posterior gradient. The scatterplots were drawn using the ChiPlot (https://www.chiplot.online/).

analysis, we first identified the principal functional gradients in the neonatal brains and their development with age during the third trimester. Then, we employed support vector regression analysis to examine whether the functional connectome gradients at birth could predict individual cognitive outcomes at 2 years of age. An independent replication dataset comprising 486 neonates aged 28–45 PMW at the time of scanning, obtained from the Developing Human Connectome Project (see the supporting information for details), was used to validate our main results.

RESULTS

The emergence of sensorimotor-to-visual gradient during the late preterm period

To qualitatively delineate the development of the sensorimotor-to-visual gradient, we conducted a cross-participant sliding window analysis to investigate changes in connectome gradients across age windows. We first divided all neonates into 15 overlapping age windows, ranging from 33.8 to 40.2 PMW, in ascending order of age. Each window comprised 10 neonates with a step size of two, meaning that window 1 included neonates 1–10, window 2 included neonates 3–12, and so forth until window 15 included neonates 29–39. We then identified a group-level connectome gradient within each age window based on the averaged functional connectivity matrix. As the first two gradients account for most of the variance of functional connectome (22.49%–36.06%), the present study focuses on the development of the first two gradients during the third trimester. When visually inspecting the first two gradients across age windows, we observed that the dominance of the sensorimotor-to-visual gradient emerged in the late preterm age window, such as 35.6 PMW, as indicated by the first maximum separation of sensorimotor and visual regions along the first gradient axis (Figure 1A, *left*). Before this critical age window, the voxels within the sensorimotor area and visual cortex showed undifferentiated locations, lacking the clear separation observed in the later age windows (Figure 1A, *left*). The cortical mapping for the first two gradients of each age window further confirmed this significant period (Figure 1A, *right*). Moreover, the secondary gradient exhibited an anterior-to-posterior pattern across the cortex at the late preterm period (Figure 1A, *left*). Additionally, we observed that the ranges of both the sensorimotor-to-visual and the anterior-to-posterior gradients gradually extended with development from the late preterm to term age (Figure 1A, *left*).

To gain insights into the gradient changes across age windows, we calculated the maturation index (i.e., the similarity to the gradients of the oldest age window) and the global measures of core connectome gradients across age windows, including the explanation ratio (i.e., accounting for the variance of the high-dimensional functional connectome), the gradient range (i.e., difference between the values of the positive and negative extremes of the gradient axis), and the gradient variation (i.e., the standard deviation of the values of the gradient axis). The sensorimotor-to-visual gradient exhibited substantial increases in the maturation indexes, explanation ratio, gradient range, and gradient variation (Figure 1B) from the late preterm (e.g., 36.5 PMW) to term age. Notably, the secondary gradient, i.e., the anterior-to-posterior gradient, demonstrated modest incremental changes across the age windows, as reflected by these three measures (Figure 1B).

To validate these qualitative results of the sensorimotor-to-visual gradient, we conducted a similar cross-participant sliding window analysis using the Replication Dataset (92 age windows; each window comprised 30 neonates with a step size of five). When visually examining the first two gradients across age windows, we observed that the dominance of the sensorimotor-to-visual gradient emerges at the late preterm age window (around 34.2 PMW, Figure S1). Taken together, these qualitative analyses provide evidence that the core sensorimotor-to-visual gradients emerge during the late preterm period (around 34 to 36 postmenstrual weeks) and undergo continuous development toward a more full-term like pattern.

The sensorimotor-to-visual gradient exhibits global and regional development during the third trimester

To quantify the developmental changes in core connectome gradients during the third trimester, we used a general linear model to assess the effect of age on the global measures and regional scores of the first two gradients, with gender and head movement parameters included as covariates.

For the principal sensorimotor-to-visual gradient, we observed significant age-related increases during the third trimester in the maturation index ($t = 5.02$, $p = 0.0001$, Figure 2A) and all global measures (explanation ratio: $t = 3.55$, $p = 0.009$; gradient range: $t = 5.67$, $p < 0.0001$; gradient variation: $t = 5.05$, $p = 0.0001$, Figure 2A). For the secondary anterior-to-posterior gradient, we only found a significant age-related increase in the maturation index ($t = 3.85$, $p = 0.004$, Figure 2B). All p values were corrected by Bonferroni corrected-$P < 0.05$.

Voxel-wise statistical analysis revealed age-associated increases in regional gradient scores of sensorimotor-to-visual mainly concentrated in the primary sensorimotor regions, involving the supplementary motor cortex and postcentral gyrus, and age-associated decreases in the inferior parietal lobe and precuneus (voxel-level $p < 0.001$, Gaussian random field cluster-level corrected $p < 0.05$, Figure 2C). For the anterior-to-posterior gradient, we did not observe significant age effects in the regional scores.

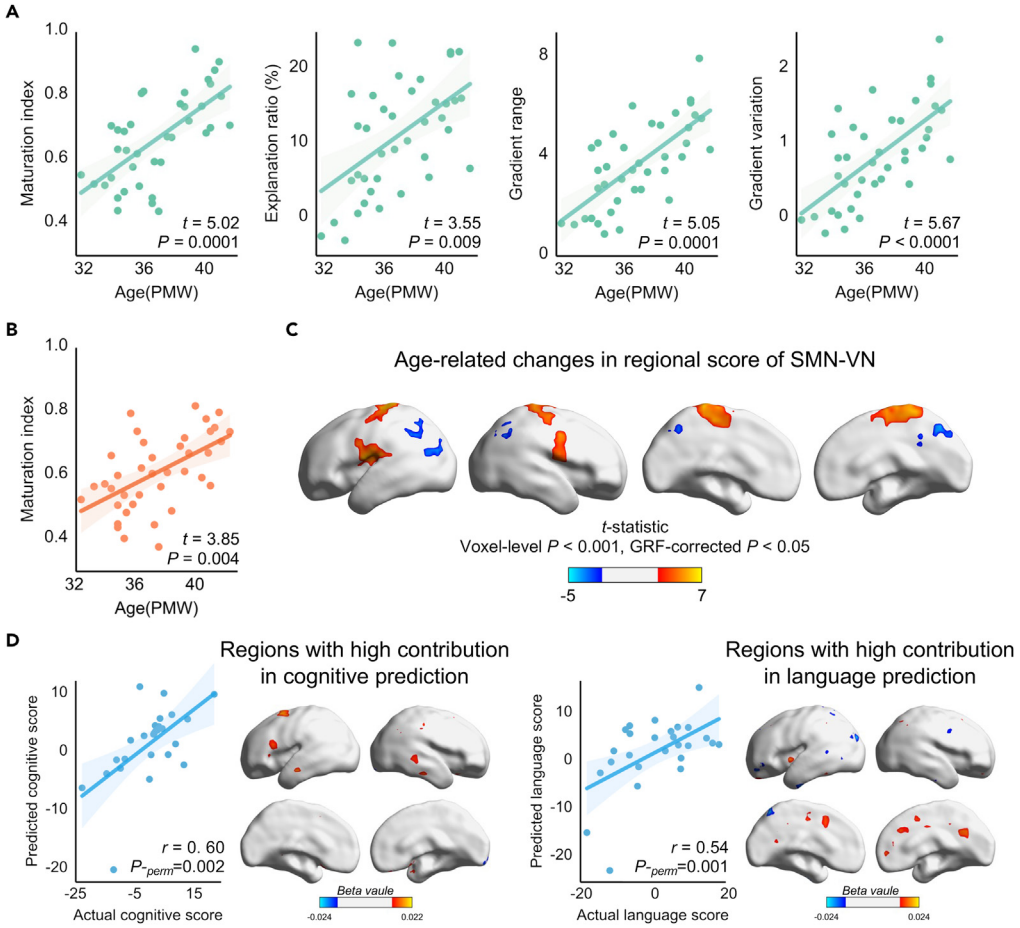

Figure 2. Connectome gradient development during the third trimester and its prediction of neurocognitive outcomes at 2 years of age

(A) Age-related increases were observed in the maturation index and all global measures of the sensorimotor-to-visual gradient, with gender and head movement parameters included as covariates.

(B) Age-related increase was observed in the maturation index of anterior-to-posterior gradient, with gender and head movement parameters included as covariates.

(C) At the regional level, gradient scores that increased with age were mostly found within the sensorimotor regions (shown in warm colors), while gradient scores in the inferior parietal lobe and precuneus decreased with age (shown in cool colors) (voxel-level $p < 0.001$, Gaussian random field (GRF) cluster-level corrected $p < 0.05$). SMN-VN, the sensorimotor-to-visual gradient.

(D) The sensorimotor-to-visual gradient from neonates significantly predicts cognitive (*left*) and language (*right*) component scores at 2 years of age. The scatterplot shows a significant Pearson correlation between actual scores and predicted scores, and the correlation coefficient was corrected by the permutation test (1,000 times). The feature contribution weights of voxels were projected on a cortical surface. The positive value indicates a positive association between regional gradient scores and behavioral scores, while the negative value represents a negative relationship. The scatterplots were drawn using the ChiPlot (https://www.chiplot.online/).

In the Replication Dataset, similar significant developmental effects were observed for the maturation index ($t = 17.73$, $p < 0.0001$, Figure S2A), global measures (gradient range: $t = 10.95$, $p < 0.0001$; gradient variation: $t = 7.11$, $p < 0.0001$, Figure S2A), and regional measures of the sensorimotor-to-visual gradient (voxel-level $p < 0.001$, Gaussian random field cluster-level corrected $p < 0.05$, Figure S2B). In addition, we also observed significant age effects in the global measures and regional gradient scores of the primary-to-transmodal gradient (Figures S2A and S2B).

Sensorimotor-to-visual gradient at birth predicts cognitive outcomes at 2 Years of age

To investigate whether functional connectome gradients in the neonatal brain predict individual neurocognitive performance later in life, we employed support vector regression with a 5-fold cross-validation approach. Specifically, we examined whether the regional score of the sensorimotor-to-visual gradient could effectively predict individual neurocognitive scores at 2 years of age (cognitive, language, and motor scores). In this analysis, we trained models using the whole-brain gradient scores and empirical neurocognitive scores of 21 newborns, leaving

out 5 neonates at a time and including scan age, sex, head motion, and time interval between scan age and birth age as covariates. We then used these trained models to predict the three neurocognitive scores for each newborn. Notably, among the three neurocognitive scores, we observed significant associations between the predicted cognitive component (r = 0.60, *P-perm* = 0.002, Figure 2D, *left*) and language component (r = 0.54, *P-perm* = 0.001, Figure 2D, *right*) scores and the empirical scores, indicating a reliable prediction of neurodevelopmental performance at 2 years of age based on the core connectome gradient in the neonatal brain. Moreover, we projected the feature contribution of each voxel onto the cortical surface and found that voxels with higher contributions to cognition were predominantly located in primary sensorimotor, auditory, and visual areas (Figure 2D, *left*), whereas voxels with higher contributions to language were predominantly localized in the insula, posterior cingulate cortex, precuneus, and visual association cortex (Figure 2D, *right*). However, the regional score of the sensorimotor-to-visual gradient could not predict the motor component scores of individuals at 2 years of age (motor: r = 0.37, *P-perm* = 0.06). In addition, the regional score of the anterior-to-posterior gradient did not predict all neurocognitive performance at 2 years of age (cognitive: r = 0.20, *P-perm* = 0.16; language: r = 0.28, *P-perm* = 0.09; motor: r = 0.19, *P-perm* = 0.19).

In the Replication Dataset, the regional score of the sensorimotor-to-visual gradient significantly predicted individual cognition (r = 0.11, *P-perm* = 0.02, Figure S3A), language (r = 0.10, *P-perm* = 0.03, Figure S3A), and motor scores (r = 0.18, *P-perm* < 0.001, Figure S3A) at 18 months of age. Moreover, the regional score of the primary-to-transmodal gradient also effectively predicted individual cognitive, language, and motor scores at 18 months of age (Figure S3B).

Taken together, these results highlight the role of the core connectome gradients at birth in shaping postnatal cognitive growth.

DISCUSSION

Our study shows for the first time the emergence and evolution of the core functional connectome gradient throughout the third trimester and establishes links between the connectome gradients in the neonatal brain and neurocognitive function at two years of age. Our main results were replicated using an independent dataset. These findings provide valuable insights into the early development of the sensorimotor-to-visual gradient and enhance our understanding of how functional brain organization develops during pregnancy to support cognitive development in later stages of life.

Although a prior study has demonstrated the existence of the sensorimotor-to-visual gradient in term-born neonatal brains,[7] our study is the first to identify the emergence of the sensorimotor-to-visual gradient at the late preterm period (34–36 PMW) and highlight the age-related changes in this gradient during the third trimester. Notably, previous studies have also observed an abrupt increase in myelinated white matter across the whole brain,[16,17,23] and a rapid enhancement in the association between individual variability and the strength of functional connectivity[24] at approximately 36 postmenstrual weeks. In conjunction with previous studies, we speculate that the late preterm is a crucial time point for the prenatal development of structural and functional brain organizations, which supports the formation of core gradients of functional connectome. In addition, during the third trimester, the sensorimotor-to-visual gradient shows age-associated increases in the explanation ratio, global topography, and spatial variation, as well as increased gradient scores in the sensorimotor regions. During this period, the sensorimotor regions involved in basic survival functions,[25] also undergo remarkable developmental changes. Classical neuroanatomy studies have reproducibly reported the priority of maturation in the cytoarchitecture and myeloarchitecture of primary sensory and motor cortices before birth.[18–20] On the other hand, numerous task-free fMRI studies have indicated that the primary cortex exhibited remarkable increases in the number and strength of functional connectivity, gradually forming an adult-like functional system as well as serving as the hub nodes of the functional brain network.[11,12,26–28] Collectively, the emergence and extension of the sensorimotor-to-visual gradient could be attributable to the gradual maturation of the primary cortex during the third trimester.

In the first 2 years of life, infants gradually develop gross motor and fine motor skills, learn to understand and use words, recognize objects, and form social and self-concepts.[29,30] The development of individual mental functions is thought to be a consequence of the maturation of human brain structure and function.[31,32] Previous studies suggest that the individual cognitions at two years of age are robustly predicted by neonatal white matter structures and cortical morphological features.[33,34] The present study highlights that the sensorimotor-to-visual gradient in the functional connectome at birth is a good predictor of cognitive and language scores at two years of age. These results form a consensus that the establishment of brain functional organization during the third trimester has important implications for postnatal cognitive growth. The sensorimotor-to-visual gradient describes the spatial variation in functional connectivity profiles across the cortex, highlighting the functional segregation between sensorimotor regions and the visual cortex.[1,7] During the third trimester, this increasing segregation in the gradient axis between the sensorimotor and visual regions may prioritize information and communication within specific modality regions, which is essential for infants' cognitive growth. Interestingly, the sensorimotor-to-visual gradient predicts the cognitive and language scores but not motor scores at 2 years of age. A plausible explanation is that the establishment of the sensorimotor-to-visual gradient not only enables the sensory-specific functions at birth,[25] but also the global efficient integration of multimodal information, which supports the maturation of infants' cognitive abilities. Moreover, the anterior-to-posterior gradient, which was already evident at around 34 postmenstrual weeks, was not found to be associated with the cognitive growth in the first 2 years. This gradient, which is widely observed in the mammalian brain, could be related to the temporal differences in neurogenesis, reflecting the homology of the human brain.[35–37]

Limitations of the study

Several issues need to be considered. Firstly, previous research has indicated rapid changes in the structural connectome of the human brain during the preterm period,[38] and the sensorimotor-to-visual gradient has been closely linked to cortical morphology and white matter

microstructures in term-born brains.[7] Our current study delineates the developmental process of core gradients in functional connectome during the third trimester. However, the relationship between the development of functional gradients and structural organization prior to birth still requires further investigation. Secondly, preterm neonates, compared to term-born infants, experience premature exposure to the external environment and are at higher risk of abnormal neurodevelopment and functional organization.[26,39] Future studies utilizing advancing fetal imaging technologies may help mitigate the impact of preterm birth on the development of brain functional gradients, thereby providing a more comprehensive understanding of longitudinal developmental trajectories *in utero*.[40] Finally, our results are highly replicated between two independent datasets. However, there are some inconsistencies between the discovery dataset and the replication datasets, such as the exact age windows for the emergence of the sensorimotor-to-visual gradient. This could be due to sample heterogeneity and the possible influence of preterm birth. Future multisite baby brain imaging studies with a larger sample size will contribute to stronger evidence in this regard.

STAR★METHODS

Detailed methods are provided in the online version of this paper and include the following:

- KEY RESOURCES TABLE
- RESOURCE AVAILABILITY
  - Lead contact
  - Materials availability
  - Data and code availability
- EXPERIMENTAL MODEL AND STUDY PARTICIPANT DETAILS
  - Participants
  - Follow-up neurodevelopmental assessments
- METHOD DETAILS
  - Image acquisition and preprocessing
  - Connectome gradient analysis
- QUANTIFICATION AND STATISTICAL ANALYSIS
  - General linear model
  - Prediction of the follow-up neurocognitive scores
- ADDITIONAL RESOURCES

SUPPLEMENTAL INFORMATION

Supplemental information can be found online at https://doi.org/10.1016/j.isci.2024.108981.

ACKNOWLEDGMENTS

The work was supported by the National Natural Science Foundation of China (31830034, 82021004, and 82102131), the National Key Research and Development Project (2018YFA0701402), and the National Institutes of Health (Grant Nos. R01MH092535, R01MH125333, R01EB031284, R01MH129981, R21MH123930, and P50HD105354). We also thank the Developing Human Connectome Project for providing the publicly available neonatal brain MRI and behavioral data for the validation analysis. Data were provided by the developing Human Connectome Project, KCL-Imperial-Oxford Consortium, funded by the European Research Council under the European Union Seventh Framework Programme (FP/2007-2013)/ERC Grant Agreement no. [319456]. We are grateful to the families who generously supported this study.

AUTHOR CONTRIBUTIONS

Yunman Xia and Yong He conceptualized and designed the research. Tina Jeon, Minhui Ouyang, Lina Chalak, Nancy Rollins, and Hao Huang collected and sorted the imaging and behavioral dataset. Jianlong Zhao and Yuehua Xu performed the imaging preprocessing for the human brain MRI data. Mingrui Xia and Dingna Duan provided the methodological instructions. Yunman Xia performed the data analysis. Yunman Xia, Yong He, and Dingna Duan wrote and revised the article.

DECLARATION OF INTERESTS

The authors declare no competing interests.

Received: August 18, 2023
Revised: December 13, 2023
Accepted: January 17, 2024
Published: January 20, 2024

REFERENCES

1. Margulies, D.S., Ghosh, S.S., Goulas, A., Falkiewicz, M., Huntenburg, J.M., Langs, G., Bezgin, G., Eickhoff, S.B., Castellanos, F.X., Petrides, M., et al. (2016). Situating the default-mode network along a principal gradient of macroscale cortical organization. Proc. Natl. Acad. Sci. USA *113*, 12574–12579. https://doi.org/10.1073/pnas.1608282113.
2. Margulies, D.S., Ovadia-Caro, S., Saadon-Grosman, N., Bernhardt, B., Jefferies, B., and Smallwood, J. (2022). Cortical Gradients and Their Role in Cognition. In Encyclopedia of Behavioral Neuroscience, 2nd edition (Elsevier), pp. 242–250. https://doi.org/10.1016/B978-0-12-819641-0.00010-4.
3. Bethlehem, R.A.I., Paquola, C., Seidlitz, J., Ronan, L., Bernhardt, B., Consortium, C.-C., and Tsvetanov, K.A. (2020). Dispersion of functional gradients across the adult lifespan. Neuroimage *222*, 117299. https://doi.org/10.1016/j.neuroimage.2020.117299.
4. Wang, J., Zhou, Y., Ding, J., and Xiao, J. (2021). Functional gradient alteration in individuals with cognitive vulnerability to depression. J. Psychiatr. Res. *144*, 338–344. https://doi.org/10.1016/j.jpsychires.2021.10.024.
5. Dong, D., Yao, D., Wang, Y., Hong, S.-J., Genon, S., Xin, F., Jung, K., He, H., Chang, X., Duan, M., et al. (2023). Compressed sensorimotor-to-transmodal hierarchical organization in schizophrenia. Psychol. Med. *53*, 771–784. https://doi.org/10.1017/S0033291721002129.
6. Xia, M., Liu, J., Sun, X., Ma, Q., Wang, X., Wei, D., Chen, Y., Liu, B., Huang, C.-C., Zheng, Y., et al. (2020). Large-scale Gradient Dysfunction of the Functional Connectome in Major Depression. Preprint at bioRxiv. https://doi.org/10.1101/2020.10.24.352153.
7. Larivière, S., Vos de Wael, R., Hong, S.-J., Paquola, C., Tavakol, S., Lowe, A.J., Schrader, D.V., and Bernhardt, B.C. (2020). Multiscale structure–function gradients in the neonatal connectome. Cereb. Cortex *30*, 47–58. https://doi.org/10.1093/cercor/bhz069.
8. Yu, Q., Ouyang, A., Chalak, L., Jeon, T., Chia, J., Mishra, V., Sivarajan, M., Jackson, G., Rollins, N., Liu, S., and Huang, H. (2016). Structural development of human fetal and preterm brain cortical plate based on population-averaged templates. Cerebral Cortex *26*, 4381–4391.
9. Dong, H.-M., Margulies, D.S., Zuo, X.-N., and Holmes, A.J. (2021). Shifting gradients of macroscale cortical organization mark the transition from childhood to adolescence. Proc. Natl. Acad. Sci. USA *118*, e2024448118. https://doi.org/10.1073/pnas.2024448118.
10. Xia, Y., Xia, M., Liu, J., Liao, X., Lei, T., Liang, X., Zhao, T., Shi, Z., Sun, L., Chen, X., et al. (2022). Development of functional connectome gradients during childhood and adolescence. Sci. Bull. *67*, 1049–1061. https://doi.org/10.1016/j.scib.2022.01.002.
11. Yu, Q., Ouyang, M., Detre, J., Kang, H., Hu, D., Hong, B., Fang, F., Peng, Y., and Huang, H. (2023). Infant brain regional cerebral blood flow increases supporting emergence of the default-mode network. Elife *12*, e78397.
12. Cao, M., He, Y., Dai, Z., Liao, X., Jeon, T., Ouyang, M., Chalak, L., Bi, Y., Rollins, N., Dong, Q., and Huang, H. (2017). Early development of functional network segregation revealed by connectomic analysis of the preterm human brain. Cereb. Cortex *27*, 1949–1963. https://doi.org/10.1093/cercor/bhw038.
13. Ouyang, M., Jeon, T., Sotiras, A., Peng, Q., Mishra, V., Halovanic, C., Chen, M., Chalak, L., Rollins, N., Roberts, T.P.L., et al. (2019). Differential cortical microstructural maturation in the preterm human brain with diffusion kurtosis and tensor imaging. Proc. Natl. Acad. Sci. USA *116*, 4681–4688. https://doi.org/10.1073/pnas.1812156116.
14. Rakic, P. (1995). Radial versus tangential migration of neuronal clones in the developing cerebral cortex. Proc. Natl. Acad. Sci. USA *92*, 11323–11327. https://doi.org/10.1073/pnas.92.25.11323.
15. Sidman, R.L., and Rakic, P. (1973). Neuronal migration, with special reference to developing human brain: a review. Brain Res. *62*, 1–35. https://doi.org/10.1016/0006-8993(73)90617-3.
16. Ouyang, M., Dubois, J., Yu, Q., Mukherjee, P., and Huang, H. (2019). Delineation of early brain development from fetuses to infants with diffusion MRI and beyond. Neuroimage *185*, 836–850.
17. Huang H: Imaging infant brain. Oxford Research Encyclopedia of Psychology. Oxford Research Encyclopedia, September 2022 Notes: https://doi.org/10.1093/acrefore/9780190236557.013.820
18. Kostović, I., and Jovanov-Milosević, N. (2006). The development of cerebral connections during the first 20-45 weeks' gestation. Semin. Fetal Neonatal Med. *11*, 415–422. https://doi.org/10.1016/j.siny.2006.07.001.
19. Huttenlocher, P.R., and Dabholkar, A.S. (1997). Regional differences in synaptogenesis in human cerebral cortex. J. Comp. Neurol. *387*, 167–178.
20. Huttenlocher, P.R. (1990). Morphometric study of human cerebral cortex development. Neuropsychologia *28*, 517–527. https://doi.org/10.1016/0028-3932(90)90031-I.
21. Rabinowicz, T. (1986). The Differentiated Maturation of the Cerebral Cortex. In Postnatal Growth Neurobiology, F. Falkner and J.M. Tanner, eds. (Springer US), pp. 385–410. https://doi.org/10.1007/978-1-4899-0522-2_14.
22. van den Heuvel, M.P., Kersbergen, K.J., de Reus, M.A., Keunen, K., Kahn, R.S., Groenendaal, F., de Vries, L.S., and Benders, M.J.N.L. (2015). The Neonatal Connectome During Preterm Brain Development. Cereb. Cortex *25*, 3000–3013. https://doi.org/10.1093/cercor/bhu095.
23. Hüppi, P.S., Warfield, S., Kikinis, R., Barnes, P.D., Zientara, G.P., Jolesz, F.A., Tsuji, M.K., and Volpe, J.J. (1998). Quantitative magnetic resonance imaging of brain development in premature and mature newborns. Ann. Neurol. *43*, 224–235. https://doi.org/10.1002/ana.410430213.
24. Xu, Y., Cao, M., Liao, X., Xia, M., Wang, X., Jeon, T., Ouyang, M., Chalak, L., Rollins, N., Huang, H., and He, Y. (2019). Development and Emergence of Individual Variability in the Functional Connectivity Architecture of the Preterm Human Brain. Cereb. Cortex *29*, 4208–4222. https://doi.org/10.1093/cercor/bhy302.
25. Buckner, R.L., and Krienen, F.M. (2013). The evolution of distributed association networks in the human brain. Trends Cognit. Sci. *17*, 648–665. https://doi.org/10.1016/j.tics.2013.09.017.
26. Eyre, M., Fitzgibbon, S.P., Ciarrusta, J., Cordero-Grande, L., Price, A.N., Poppe, T., Schuh, A., Hughes, E., O'Keeffe, C., Brandon, J., et al. (2021). The Developing Human Connectome Project: typical and disrupted perinatal functional connectivity. Brain *144*, 2199–2213. https://doi.org/10.1093/brain/awab118.
27. Fransson, P., Skiöld, B., Horsch, S., Nordell, A., Blennow, M., Lagercrantz, H., and Aden, U. (2007). Resting-state networks in the infant brain. Proc. Natl. Acad. Sci. USA *104*, 15531–15536. https://doi.org/10.1073/pnas.0704380104.
28. Fransson, P., Aden, U., Blennow, M., and Lagercrantz, H. (2011). The functional architecture of the infant brain as revealed by resting-state fMRI. Cereb. Cortex *21*, 145–154. https://doi.org/10.1093/cercor/bhq071.
29. Berk, L. (2015). Child Development (Pearson Higher Education AU).
30. Rochat, P., Broesch, T., and Jayne, K. (2012). Social awareness and early self-recognition. Conscious. Cognit. *21*, 1491–1497. https://doi.org/10.1016/j.concog.2012.04.007.
31. Casey, B.J., Tottenham, N., Liston, C., and Durston, S. (2005). Imaging the developing brain: what have we learned about cognitive development? Trends Cognit. Sci. *9*, 104–110. https://doi.org/10.1016/j.tics.2005.01.011.
32. Johnson, M.H. (2005). Developmental Cognitive Neuroscience: An Introduction, 2nd ed (Blackwell Publishing).
33. Li, Y., Cheng, J., Zhang, X., Fang, R., Liao, L., Ding, X., Ni, H., Xu, X., Wu, Z., Hu, D., et al. (2021). Learning Infant Brain Developmental Connectivity for Cognitive Score Prediction. In Machine Learning in Medical Imaging Lecture Notes in Computer Science, C. Lian, X. Cao, I. Rekik, X. Xu, and P. Yan, eds. (Springer International Publishing), pp. 228–237. https://doi.org/10.1007/978-3-030-87589-3_24.
34. Ouyang, M., Peng, Q., Jeon, T., Heyne, R., Chalak, L., and Huang, H. (2020). Diffusion-MRI-based regional cortical microstructure at birth for predicting neurodevelopmental outcomes of 2-year-olds. Elife *9*, e58116. https://doi.org/10.7554/eLife.58116.
35. Cahalane, D.J., Charvet, C.J., and Finlay, B.L. (2012). Systematic, balancing gradients in neuron density and number across the primate isocortex. Front. Neuroanat. *6*, 28. https://doi.org/10.3389/fnana.2012.00028.
36. Elston, G.N. (2000). Pyramidal Cells of the Frontal Lobe: All the More Spinous to Think With. J. Neurosci. *20*, RC95. https://doi.org/10.1523/JNEUROSCI.20-18-j0002.2000.
37. Rakic, P. (2002). Neurogenesis in adult primate neocortex: an evaluation of the evidence. Nat. Rev. Neurosci. *3*, 65–71. https://doi.org/10.1038/nrn700.
38. Zhao, T., Mishra, V., Jeon, T., Ouyang, M., Peng, Q., Chalak, L., Wisnowski, J.L., Heyne, R., Rollins, N., Shu, N., and Huang, H. (2019). Structural network maturation of the preterm human brain. Neuroimage *185*, 699–710. https://doi.org/10.1016/j.neuroimage.2018.06.047.
39. Ball, G., Srinivasan, L., Aljabar, P., Counsell, S.J., Durighel, G., Hajnal, J.V., Rutherford, M.A., and Edwards, A.D. (2013). Development of cortical microstructure in the preterm human brain. Proc. Natl. Acad. Sci.

USA *110*, 9541–9546. https://doi.org/10.1073/pnas.1301652110.

40. Studholme, C. (2011). Mapping Fetal Brain Development in utero Using MRI: The Big Bang of Brain Mapping. Annu. Rev. Biomed. Eng. *13*, 345–368. https://doi.org/10.1146/annurev-bioeng-071910-124654.
41. Yan, C.-G., Wang, X.-D., Zuo, X.-N., and Zang, Y.-F. (2016). DPABI: Data Processing & Analysis for (Resting-State) Brain Imaging. Neuroinformatics *14*, 339–351. https://doi.org/10.1007/s12021-016-9299-4.
42. Wang, J., Wang, X., Xia, M., Liao, X., Evans, A., and He, Y. (2015). GRETNA: a graph theoretical network analysis toolbox for imaging connectomics. Front. Hum. Neurosci. *9*, 458.
43. Makropoulos, A., Robinson, E.C., Schuh, A., Wright, R., Fitzgibbon, S., Bozek, J., Counsell, S.J., Steinweg, J., Vecchiato, K., Passerat-Palmbach, J., et al. (2018). The developing human connectome project: A minimal processing pipeline for neonatal cortical surface reconstruction. Neuroimage *173*, 88–112. https://doi.org/10.1016/j.neuroimage.2018.01.054.
44. Bayley, N. (2006). Bayley Scales of Infant and Toddler Development (Harcourt Assessment, Psych. Corp).
45. Serag, A., Aljabar, P., Ball, G., Counsell, S.J., Boardman, J.P., Rutherford, M.A., Edwards, A.D., Hajnal, J.V., and Rueckert, D. (2012). Construction of a consistent high-definition spatio-temporal atlas of the developing brain using adaptive kernel regression. Neuroimage *59*, 2255–2265. https://doi.org/10.1016/j.neuroimage.2011.09.062.
46. Yan, C.-G., Craddock, R.C., He, Y., and Milham, M.P. (2013). Addressing head motion dependencies for small-world topologies in functional connectomics. Front. Hum. Neurosci. *7*, 910. https://doi.org/10.3389/fnhum.2013.00910.
47. Hughes, E.J., Winchman, T., Padormo, F., Teixeira, R., Wurie, J., Sharma, M., Fox, M., Hutter, J., Cordero-Grande, L., Price, A.N., et al. (2017). A dedicated neonatal brain imaging system. Magn. Reson. Med. *78*, 794–804. https://doi.org/10.1002/mrm.26462.
48. Salimi-Khorshidi, G., Douaud, G., Beckmann, C.F., Glasser, M.F., Griffanti, L., and Smith, S.M. (2014). Automatic denoising of functional MRI data: combining independent component analysis and hierarchical fusion of classifiers. Neuroimage *90*, 449–468. https://doi.org/10.1016/j.neuroimage.2013.11.046.
49. Coifman, R.R., Lafon, S., Lee, A.B., Maggioni, M., Nadler, B., Warner, F., and Zucker, S.W. (2005). Geometric diffusions as a tool for harmonic analysis and structure definition of data: Diffusion maps. Proc. Natl. Acad. Sci. USA *102*, 7426–7431. https://doi.org/10.1073/pnas.0500334102.
50. Langs, G., Golland, P., and Ghosh, S. (2015). Predicting activation across individuals with resting state functional connectivity based multi-atlas label fusion, pp. 313–320. https://doi.org/10.1007/978-3-319-24571-3_38.
51. Mardia, K.V., Kent, J.T., and Bibby, J.M. (2006). Multivariate Analysis Tranferred to Digital Pr (Acad. Press).

STAR★METHODS

KEY RESOURCES TABLE

REAGENT or RESOURCE	SOURCE	IDENTIFIER
Human T2-weighted structural MRI and resting-state functional MRI data	Developing Human Connectome Project	http://www.developingconnectome.org/
Software and algorithms		
Neonatal gradient development code	This paper	https://doi.org/10.5281/zenodo.10431700
Connectome gradient analysis	Margulies et al.[1]	https://doi.org/10.1016/B978-0-12-819641-0.00010-4
Data Processing & Analysis for (Resting-State) Brain Imaging (DPABI) toolbox	Yan et al.[41]	https://doi.org/10.1007/s12021-016-9299-4
GRETNA 2.0	Wang et al.[42]	https://doi.org/10.3389/fnhum.2015.00386
SPM12	Welcome Department of Cognitive Neurology, London, UK	www.fil.ion.ucl.ac.uk/spm
Other		
Bayley Scales of Infant and Toddler Development-third edition	San Antonio, TX: Harcourt Assessment, Inc.	https://doi.org/10.1177/0734282906297199.

RESOURCE AVAILABILITY

Lead contact

Further information and requests for resources should be directed to and will be fulfilled by the lead contact, Yong He, Ph.D., E-mail: yong.he@bnu.edu.cn.

Materials availability

This study did not generate new unique reagents.

Data and code availability

- All statistical data used in the exploration analysis will be shared by the lead contact upon request. The data used in the validation analysis is existing, publicly available data (Developing Human Connectome Project). The accession link for the datasets is listed in the key resources table.
- The code used in this work has been deposited at Zenodo and is publicly available as of the date of publication. DOIs are listed in the key resources table.
- Any additional information required to reanalyze the data reported in this paper is available from the lead contact upon request.

EXPERIMENTAL MODEL AND STUDY PARTICIPANT DETAILS

Participants

We collected resting-state fMRI data from 52 neonates recruited from Parkland Memorial Hospital in Dallas. A neonatologist and an experienced pediatric neuroradiologist screened the neonatal ultrasound and clinical MRI data as well as the neonatal and mothers' medical records. Specific exclusion criteria were introduced in our previous studies.[24,38] Besides, we also performed a quality control for brain imaging data and then excluded 13 neonates considering their excessive head motion. Finally, we performed further analysis using data from 39 neonates (Female/Male = 11/28, postmenstrual age at birth: 33.2 $\pm$ 4.5 weeks, range 25.1–40.7 weeks; postmenstrual age at scan: 37.0 $\pm$ 2.7 weeks, range 31.3–41.7 weeks, Black/White = 7/32, Hispanic/non-Hispanic = 28/11). For each neonate, we obtained written and informed parental consents from neonatal parents. And this study was approved by the Institutional Review Board of the University of Texas Southwestern Medical Center.

For validation purposes, we utilized a Replication Dataset derived from the Developing Human Connectome Project (dHCP) project (http://www.developingconnectome.org/).[43] This project included longitudinal MRI scans from 783 healthy neonates, which were conducted at the Newborn Imaging Center at Evelina London Children's Hospital, London, UK. Meanwhile, this project obtained ethical approval (14/LO/1169), and written informed consent from the parents/guardians of all neonates. We conducted strict quality control procedures for each fMRI scans in the dHCP dataset before inclusion in further analysis. Consequently, 297 neonates were excluded due to various reasons,

including low radiological scores (exceed 2) (N = 156), failure to pass fMRI quality control (N = 66), sedation or lack of fMRI files (N = 6), excessive head motion (N = 60), and poor registration quality (N = 9). After this rigorous quality control process, we specifically selected the earliest session for each neonate, resulting in a Replication Dataset comprising 486 scans from 486 neonates (Female/Male = 216/270, aged 28–45 postmenstrual weeks at scanning, and aged 24–43 postmenstrual weeks at birth). The dHCP dataset does not release information on ancestry, race, or ethnicity.

Follow-up neurodevelopmental assessments

Among the 39 neonates used in further exploration analyses, we only collected the follow-up neurodevelopmental assessments from 26 neonates (Female/Male = 7/19, postmenstrual age at scan: 36.7 $\pm$ 2.8 weeks) at age of 2 years (chronological age at assessment: 23.5 $\pm$ 2.3 months). We assessed individual neurodevelopment using Bayley Scales of Infant and Toddler Development-third edition, including cognitive component scale, language component scale, and motor component scale.[44] The Bayley Scale III is a widely used standardized tool to assess the development of multiple dimensional functions of infants and toddlers. Specifically, the cognitive component scale assesses the non-verbal general cognitive ability, including exploration and manipulation, object relatedness, concept formation, and memory; the language component scale estimates the abilities including receptive and expressive communication through words and gestures; the motor component scale measures the development of gross and fine motor.[44] On the other hand, to avoid the Hawthorne effect, we asked a certified neurodevelopmental psychologist, who was unknown of the clinical conditions of neonates, to conduct the assessments for all toddlers.

Within the Replication Dataset, 385 neonates underwent neurodevelopmental assessments at 18 months, using the same measurement tool employed in the discovery analysis, that is the Bayley Scales of Infant and Toddler Development-third edition.[44] These assessments were carried out by two skilled assessors at St. Thomas' Hospital, London. Furthermore, to prevent information leakage during the predictive process, we retained only one neonate from each pair of twins, resulting in the exclusion of 21 neonates. Finally, 364 neonates were used to explore whether functional connectome gradients in neonatal brains can predict individual neurocognitive performance later in life.

METHOD DETAILS

Image acquisition and preprocessing

All neonates in the exploration dataset were scanned with identical protocols using a single scanner. After neonates were naturally sleep, high-resolution T2-weighted (T2w) images and rs-fMRI data for each neonate were acquired using a Philips 3.0 T Achieva MR scanner at the Children's Medical Center, Dallas. All neonates were fed before the MRI scan and securely wrapped in a vacuum immobilizer to minimize motion. Earplugs, earphones, and extra foam padding were utilized to diminish the scanner noise. If the baby wakes up, the scan is stopped. Parameters for the T2w scans were as follows: repetition time (TR) = 3000 ms; echo time (TE) = 80 ms; field of view (FOV) = 168 × 168 mm^2; number of slices = 65 and voxel size = 1.5 × 1.5 × 1.6 mm^3.

These structural T2w scans were assessed by an experienced pediatric neuroradiologist to ensure that data with anatomical abnormalities were not included in the study. Instead of performing segmentation of individual structural T2w scans, we employed a publicly available 37-week brain template[45] to generate specific tissue masks. The rs-fMRI scans were performed using a T2w gradient-echo EPI sequence with the following parameters: TR = 1500 ms; TE = 27 ms; flip angle = 80°; FOV = 168 × 168 mm^2; number of slices = 30; number of volumes = 210; and voxel size = 2.4 × 2.4 × 3 mm^3. All rs-fMRI data was preprocessed using SPM12 (Welcome Department of Cognitive Neurology, London, UK; www.fil.ion.ucl.ac.uk/spm), the Data Processing & Analysis for (Resting-State) Brain Imaging (DPABI) toolbox 4.3 version,[41] and GRETNA 2.0 version[42] implemented in the MATLAB 2018b (Math Works, Natick, MA) platform.

The preprocessing of the rs-fMRI data included the following steps: (*i*) removal of the first 15 time points; (*ii*) slice timing correction; (*iii*) head motion correction and exclusion of neonates with excessive head movement (maximum head motion >5 mm or >5°, or mean frame-wise displacement >1 mm); (*iv*) normalization of functional images to the customized group-level template. Specifically, we first normalized the functional images to individual T2w structural images, and then registered the individual T2w images to a publicly 37-week brain template.[45] Then we re-registered individual T2w images using the group averaged first registered T2w image as the group-level template. Finally, the functional images were re-normalized to the group-level template using the transformation parameters from the second registration and re-sampled to a 3 mm isotropic resolution; (*v*) smoothing of the time series signal (FWHM = 4 mm); (*vi*) detrending of linear drift; and (*vii*) removal of spurious variance through linear regression. Nuisance regressors included Friston's 24 head motion parameters, white matter, cerebrospinal fluid signals, and global brain signals; (*viii*) temporal bandpass filtering (0.01–0.08 Hz); and (*ix*) scrubbing voxel-specific head motion by linear regression bad time point (FD > 0.2 mm), and exclusion of neonates with excessive bad time points (>50%).[46]

In the Replication Dataset, after neonates naturally entered sleep, high-resolution T2-weighted (T2w) images and rs-fMRI data were acquired using a 3T Philips Achieva scanner, equipped with a specifically developed 32-channel neonatal receiver coil integrated system at the Evelina Newborn Imaging Center, Evelina London Children's Hospital. Further details regarding the scanning process have been previously outlined.[47] The high-resolution T2-w images were acquired with the following parameters: repetition time (TR) = 12 000 ms, field of view (FOV) = 145 × 145 × 108 mm, echo time (TE) = 156 ms. The rs-fMRI data were obtained using the following parameters: TR = 392 ms, TE = 38 ms, flip angle = 34, voxel size = 2.15 × 2.15 × 2.15 mm^3, number of volumes = 2300, scan time = 15 min 3 s, and multiband factor = 9.

In the Replication Dataset, we used minimally preprocessed rs-fMRI images.[43] This preprocessing encompassed susceptibility distortion correction using the field maps, correction for head motion by aligning all volumes to the volume exhibiting the least motion, the two steps co-registration to the T2-w image, and ICA denoising utilizing FSL FIX.[48] Subsequently, the rs-fMRI images were further preprocessed using

SPM12, DPABI, and GRETNA following same procedures employed in the discovery analysis, except that scrubbing voxel-specific head motion by linear regression bad time point (FD > 0.5 mm).

Connectome gradient analysis

For each neonate, we performed connectome gradient analyses followed the method proposed by Margulies et al.[1] In this method, functional gradients represent the degree of similarity of the functional connectivity profiles between different brain regions, with regions showing more similar connectivity profiles located closer along the gradient axes.[1] We first obtained a voxel-wise functional connectivity matrix (6,096 × 6,096) for each individual by calculating the Pearson correlation coefficient between the BOLD time series of each pair of gray matter nodes (without sub-cortical tissues). To avoid the noise of spurious connectivity, we thresholded the functional connectivity matrix of the top 10% correlation values of each voxel.[1] Then we calculated the cosine similarity between functional connectivity profiles of all pairs of voxels, and obtained a similarity matrix that represents the similarity in connectivity profiles of voxels. Next, we applied the diffusion map embedding technique[49] to dimensionally reduce the high-dimensional similarity matrix to multiple low-dimensional embedding gradients followed previous parameters.[1,10] To ensure the individual gradients were comparable, we used the Procrustes rotation approach[50] to align the original gradients of all neonates to the iterative template of term-born infants. Specifically, we first calculated the group level gradient of term-born neonates based on the group-averaged functional connectivity matrix, and then aligned raw gradients of all neonates to the group level gradient of term-born. The group-averaged aligned gradient of all neonates was taken as the gradient template for the second time alignment. We repeated this alignment process 100 times and obtained aligned gradients of each neonate. For the aligned individual gradients, we calculated the maturation index (i.e., the similarity with the gradient axis of the oldest age window) and the three global measures of the first two gradients, including explanation ratio (i.e., accounted for the variance of high-dimensional functional connectome), gradient range (i.e., difference between the values of positive and negative extremes of the gradient axis), and gradient variation (i.e., the standard deviation of values of gradient axis).

After constructing the voxel-wise functional connectivity matrix (6,905 × 6,905), we performed the identical connectome gradient analysis on the Replication Dataset. We also obtained global measures and regional scores derived from the first two gradient axes for further analysis.

QUANTIFICATION AND STATISTICAL ANALYSIS

General linear model

To investigate age-related changes in core functional connectivity gradients, we used the general linear model[51] to assess age effect on global gradient measures and regional gradient scores of first two gradients in neonates, with gender and head motion parameters (mean FD) as covariates. The general linear model is defined as follows:

$Y_g = \beta_0 + \beta_{age} \times age + \beta_{gender} \times gender + \beta_{mFD} \times mFD$,where Y_g is the connectome gradient measures of each neonate, β_{age} is the age effect. Bonferroni correction was performed to correct for multiple comparisons (8 times) across the global measures, and the Bonferroni corrected $p < 0.05$ was considered significant.

Further, to correct for multiple comparisons in the statistical analysis of regional gradient scores, we used a voxel-level threshold of $p < 0.001$ and a Gaussian Random Field (GRF) cluster-level correction of $p < 0.05$ to minimize false positive error.

Prediction of the follow-up neurocognitive scores

To investigate whether the core functional connectome gradient in neonates can predict the subsequent neurocognitive maturation, we used the support vector regression (SVR) method with a linear kernel function to examine the prediction power of neonatal functional gradients on follow-up neurocognitive scores. Prediction performance was evaluated using the 5-fold cross-validation. Specifically, each training set comprised 4/5 of all neonates and generated a classifier to predict the neurocognitive scores of the remaining neonates. The classifier operated on the regional scores of the sensorimotor-to-visual gradient. To assess the prediction accuracies of neurocognitive scores, we calculated Pearson's correlation coefficient between the actual and predicted residuals of neurocognitive scores, considering the scan age, sex, head motion parameters, and range between scan age and birth age as the covariables. The support vector regression analysis was implemented in the MATLAB 2021b (Math Works, Natick, MA) platform using a modified *fitrsvm* () function. Finally, we used the permutation test (1,000 iterations) with randomly shuffled neurocognitive scores to examine whether the prediction performance exceeded chance levels.

ADDITIONAL RESOURCES

This study did not generate or contributed to a new website/forum.